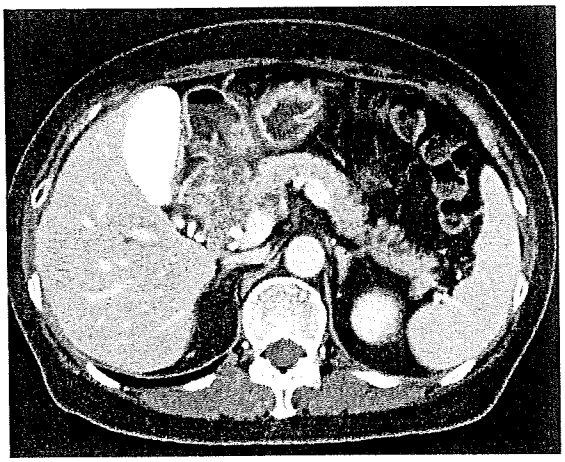

Figure 4. Abdominal computed tomography of Case 4 before treatment. The mass in the pancreatic head is contiguous with the duodenum and appears to invade the adjacent pancreatic tissue.

DISCUSSION

Surgical management remains the only curative therapy for patients with of ACC of pancreas with localized and resectable disease. Those who were treated by surgical resection were reported to show a median survival of longer than 30 months (7,8). This compares favorably with the data for patients with ductal adenocarcinoma of the pancreas; published reports on survival after resection have indicated a median survival of 12–18 months (10). More than 70% of the patients who undergo surgical resection are eventually confirmed to show recurrent disease (9). These results suggest that micrometastases are present even in cases where the disease is apparently localized to the pancreas (9).

In addition, most patients with pancreatic ACC present with unresectable locally advanced disease or obvious metastases. For patients at this stage of the disease, no adequate treatment strategies have been established yet (10,11), because no randomized controlled trials have been performed to confirm the efficacy of treatments. There are only a few reports on the use of single-drug chemotherapy, combination chemotherapy (9), chemoradiotherapy (10) or hepatic arterial injection chemotherapy (12–14) (Table 2). To the best of our knowledge, gemcitabine has never been demonstrated to show efficacy against ACC, although the drug has been widely used as the standard agent for the treatment of pancreatic adenocarcinoma. We administered chemotherapy with gemcitabine for patients with pancreatic ACC, and two of these patients showed SD without obvious tumor shrinkage. In addition, severe renal damage caused by gemcitabine was observed in one of our patients. Therefore, in our impression, chemotherapy with gemcitabine is not very promising for pancreatic ACC, although the true efficacy can only be determined by randomized controlled trials.

Some case studies have reported tumor shrinkage with fluoropyrimidine-based treatments. Holen et al. reviewed 22 chemotherapy regimens administered to 18 different patients and reported that there were no complete responses, only two PRs and seven SDs. The PRs were seen for combinations of irinotecan, 5-fluorouracil and leucovorin and also cytarabine, cisplatin and caffeine (9). It is noteworthy that ACCs of the pancreas tended to respond to 5-fluorouracil-based chemotherapies. The three patients showing PR reported in different case series had received combination therapies. Two of the patients had received 5-fluorouracil-based chemotherapy, and one patient had received combination therapies based on capecitabine (Table 2). In addition, we also observed good response to chemotherapy with S-1, a type of fluoropyrimidine. Further research is needed to clarify whether administration of fluoropyrimidine might improve the unsatisfactory results of chemotherapy for this disease.

For patients with unresectable, yet locally confined disease, radiotherapy may be one of the treatment options, as focal disease control may be expected. Holen et al. (9) also reported that all of the eight patients who were treated by radiation showed either PR or SD. Lee and Kim (10) reported two PR cases among locally advanced cases of ACC of the pancreas treated by concurrent capecitabine and radiation therapy. To obtain control of not only localized disease, but also of distant metastatic disease, radiotherapy combined with chemotherapy may be a potentially useful treatment strategy, but there are only a few reports of its use until date.

In conclusion, randomized controlled trials are needed to establish effective treatment strategies for unresectable

Table 2. Previous reports of chemotherapy or chemoradiotherapy for acinar cell carcinoma

Authors	Treatments	No. of patients	Antitumor response	Time to progression
Holen et al. (9)	5-Fluorouracil + radiation	2	PR, SD	NE
Sakon et al. (12)	Capecitabine + radiation	2	PR, PR	>15 months
Lee and Kim (10)	5-Fluorouracil[a] + mitomycin C[a] + cisplatin[a]	1	PR	18 months
Holen et al. (9)	Irinotecan + 5-fluorouracil + leucovorin	1	PR	7 months
Holen et al. (9)	Cytarabine + cisplatin + caffeine	1	PR	3 months

[a]Hepatic artery injection.

pancreatic ACC. However, it is not easy to recruit patients for trials, as pancreatic ACC is a very rarely occurring tumor. Multicenter and multinational cooperative trials are necessary to establish treatments to improve the dismal prognosis of patients with this disease.

Funding

This study was supported by a Grant-In-Aid for Cancer Research (Grant No. 20-11) from the Ministry of Health, Labour, and Welfare of Japan.

Conflict of interest statement

None declared.

References

1. Matsuno S, Egawa S, Fukuyama S, Motoi F, Sunamura M, Isaji S, et al. Pancreatic cancer registry in Japan: 20-years experience. (The national pancreatic cancer registration survey in Japan.) *Pancreas* 2004;28:219–30.
2. Cubilla AL, Fitzgeralf PJ. Tumors of the exocrine pancreas. Washington, DC: Armed Forces Institute of Pathology 1984;208–12.
3. Tatli S, Mortele KJ, Levy AD, Glickman JN, Ros PR, Banks PA, et al. CT and MRI features of pure acinar cell carcinoma of the pancreas in adults. *Am J Roentgenol* 2005;184:511–9.
4. Nasu J, Hishinuma S, Ando J, Ozawa I, Matsui J, Inadac T, et al. A case report of acinar cell carcinoma of the pancreas showing rapid growth of liver metastasis after curative pancreatectomy. *Jpn Dig Surg* 1995;28:102–6.
5. Klimstra DS, Heffess CS, Oertel JE, Rosai J. Acinar cell carcinoma of the pancreas. A clinicopathologic study of 28 cases. *Am J Surg Pathol* 1992;16:815–37.
6. Solcia E, Capella C, Kloppel G. Tumors of the exocrine pancreas. In: Rosai J, Sorbin L, editors. *Atlas of Tumor Pathology, 3rd Series, Fasc. 20.* Washington, DC: Armed Forces Institute of Pathology 1997;31–144.
7. Mulkeen AL, Yoo PS, Charles C. Less common neoplasms of the pancreas. *World J Gastroenterol* 2006;12:3180–5.
8. Tsiotos GG, Farnell MB, Sarr MG. Are the results of pancreatectomy for pancreas carcinoma improving? *World J Surg* 1999;23:913–9.
9. Holen KD, Klimstra DS, Hummer A, Gonen M, Conlon K, Brennan M, et al. Clinical characteristics and outcomes from an institutional series of acinar cell carcinoma of the pancreas and related tumors. *J Clin Oncol* 2002;20:4673–8.
10. Lee JL, Kim TW. Locally advanced acinar cell carcinoma of the pancreas successfully treated by capecitabine and concurrent radiotherapy: report of two cases. *Pancreas* 2003;27:18–22.
11. Ukei T, Okagawa K, Uemura Y. Effective intra-arterial chemotherapy for acinar cell carcinoma of the pancreas. *Dig Surg* 1999;16:76–9.
12. Sakon M, Osato H, Kishimoto S, Aoki T, Yamada T, Higaki N, et al. A patient with pancreatic acinar cell carcinoma, effectively treated by the infusion chemotherapy through hepatic artery using 5-FU, CDDP and MMC. *Jpn J Cancer Chemother* 1994;23:1614–6 (in Japanese).
13. Chen CP, Chao Y, Li CP, Lee RC, Tsay SH, Chi KH, et al. Concurrent chemoradiation is effective in the treatment of alpha-fetoprotein-producing acinar cell carcinoma of the pancreas: report of a case. *Pancreas* 2001;22:326–9.
14. Holen K, Klimstra D, Karpeh M, Conlon K, Brennan M, Saltz L, et al. Acinar cell carcinoma of the pancreas: prognostic information and treatment review from an institutional series. *Proc Am Soc Clin Oncol* 2001;20:623a.

Jpn J Clin Oncol 2009;39(12)797–806
doi:10.1093/jjco/hyp112

Regular Dose of Gemcitabine Induces an Increase in CD14$^+$ Monocytes and CD11c$^+$ Dendritic Cells in Patients with Advanced Pancreatic Cancer

Atsuko Soeda[1,2], Yuriko Morita-Hoshi[1], Hiroaki Makiyama[1], Chigusa Morizane[3], Hideki Ueno[3], Masafumi Ikeda[3], Takuji Okusaka[3], Shizuka Yamagata[1], Noriko Takahashi[1], Ichinosuke Hyodo[2], Yoichi Takaue[1] and Yuji Heike[1]

[1]Department of Medical Oncology, National Cancer Center Hospital, Tokyo, [2]Department of Gastroenterology, Institute of Clinical Medicine, University of Tsukuba, Ibaraki and [3]Hepatobiliary and Pancreatic Oncology Division, National Cancer Center Hospital, Tokyo, Japan

Received April 16, 2009; accepted August 10, 2009; published online October 1, 2009

Objective: Chemotherapy and immunotherapy often seem to contradict each other. However, recent reports suggested that the anticancer effects in some chemotherapeutic agents were concerned with immune response. This study was designed to evaluate the immunological reaction by gemcitabine for future clinical trial of combination therapy with gemcitabine and cancer vaccines.

Methods: We evaluated several immunological parameters in patients with advanced pancreatic cancer who received a conventional dose of gemcitabine for 2 months. Twenty-eight patients with metastasis or locally advanced tumor, including 18 gemcitabine-naïve and 10 with a history of preceding gemcitabine treatment, were enrolled in this study. The patients received gemcitabine 1000 mg/m^2 for 3 weeks, followed by 1 week of rest. We monitored the kinetics of lymphocytes, natural killer cells, monocytes, dendritic cells (DC), human leukocyte antigen (HLA)-multimer conjugated with CMV or WT1 peptide, and intracellular cytokine production of interferon-γ and interleukin-4 by flow cytometry. The T cell receptor (TCR) repertoire was also analyzed.

Results: The absolute number and percentage of CD14$^+$ monocytes and CD11c$^+$ (myeloid) DC increased with gemcitabine treatment ($P = 0.033$ and $P = 0.021$). The percentage of CD123$^+$ (plasmacytoid) DC also increased ($P = 0.034$), whereas no significant change was observed in other immune parameters, including multimer, intracellular cytokine production and TCR repertoire.

Conclusions: Our finding that gemcitabine treatment induced the proliferation of CD14$^+$ monocytes and CD11c$^+$ DC could support combination therapy with gemcitabine and specific immunotherapy such as peptide vaccination against pancreatic cancers.

Key words: gemcitabine – dendritic cell – monocyte – pancreatic cancer – cancer vaccines

INTRODUCTION

Pancreatic cancer remains one of the most difficult cancers to treat. It is the fifth leading cause of cancer death in Japan (1) and the fourth in both sexes in the USA (2). Although gemcitabine has been the standard treatment option for unresectable disease for the past 10 years (3), the achieved benefit is suboptimal with objective response rates of <15% and a median survival of <6 months. Many clinical trials of cytotoxic or biologic agents combined with gemcitabine have not shown any survival advantage over gemcitabine alone (4–7). In 2005, the combination of erlotinib plus gemcitabine showed a statistically significant improvement in overall survival; however, the increase in median survival was marginal (6.24 vs. 5.91 months) (8).

Gemcitabine is a nucleotide analog which inhibits DNA synthesis. It is a relatively well-tolerated drug, except that Grade 3–4 neutropenia occurs in 26% of the patients (3). Plate et al. (9) reported the effects of gemcitabine treatment

For reprints and all correspondence: Yuji Heike, Department of Medical Oncology, National Cancer Center Hospital, 5-1-1 Tsukiji Chuo-ku, Tokyo 104-0045, Japan. E-mail: yheike@ncc.go.jp

© The Author (2009). Published by Oxford University Press. All rights reserved.

on immune cells, such as immune cell numbers and their function, as determined by intracellular cytokine production and ELISPOT assays. Although the absolute number of all lymphocyte subpopulations declined during the study period, there was no significant change in the proportion of most lymphocyte subtypes, except for $CD3^+CD45RO^+$ memory lymphocytes. In their experiment, immune-monitoring was limited to 21 days during the initial course of treatment, with no follow-up evaluation. In this study, we monitored immune parameters for 2 months in gemcitabine-naïve patients and in those who had already started treatment. Our data could provide a basis for planning a clinical trial of combination therapy with gemcitabine and various immunotherapies, including cancer vaccines.

PATIENTS AND METHODS

Patients, Treatment Schedule and Sampling

After written informed consent was obtained, peripheral blood (PB) samples were obtained from patients with pancreatic cancer who were planned to receive (gemcitabine-naïve group) or who had already started gemcitabine treatment (treated group) from August 2006 to September 2007 at the National Cancer Center Hospital (Tokyo, Japan). All of them had a histological or cytological diagnosis of pancreatic adenocarcinoma. None of them had received other chemotherapeutic agents or radiation therapy except for resection of the tumor and/or intraoperative radiation therapy. The patients were treated with gemcitabine 1000 mg/m^2 for 3 weeks followed by 1 week of rest. This cycle was repeated every 4 weeks. Before each treatment, blood counts were checked, and if neutropenia ($<1000/mm^3$) developed, the treatment was suspended. None of the patients used oral steroid, but some used intravenous dexamethasone treatment (8 mg) to prevent nausea before gemcitabine injection. Ten milliliters of heparinized blood and 7 ml EDTA blood were taken on days 0 and 14 of the first course, and on the first days of the second and third courses (Fig. 1). Heparinized blood was immediately used in the FACS analysis, and EDTA blood was lysed by Buffer EL (BD Biosciences PharMingen, San Diego, CA, USA), mixed with Buffer RLT (BD Biosciences PharMingen) and cryopreserved at $-80°C$ as an RNA lysate until the T cell receptor (TCR) repertoire analysis.

Flow Cytometry for Cell Phenotyping

The fluorescent-conjugated monoclonal antibodies (MAbs) used in this study are listed in Table 1. According to the manufacturer's protocol, PB samples were incubated with MAbs for 30 min at room temperature in the dark. Red blood cells were lysed by PhamLyse (BD). After being washed (CellWash from BD), the cells were fixed (CellFix from BD) and acquired on a flow cytometer (FACSCalibur, Becton Dickinson, CA, USA). Analyses were performed using CellQuest software. We calculated the absolute number of each cell type using the following formulas:

Lymphocyte phenotypes and natural killer (NK) cells:

$$\begin{aligned}\text{Count of each phenotype (cells/}\mu\text{l)} &= \text{WBC count}^{CD} \times \%\ \text{lymphocyte fraction}^{CD} \\ &\times \%\ \text{phenotype of lymphocyte gating}^{FM}\end{aligned}$$

$CD14^+$ monocytes:

$$\begin{aligned}\text{Count (cell/}\mu\text{l)} &= \text{WBC count}^{CD} \times \%\ \text{monocyte fraction}^{CD} \\ &\times \%\ CD14^+\ \text{cells in monocyte gating}^{FM}\end{aligned}$$

Dendritic cells (DC):

$$\begin{aligned}\text{Count (cell/}\mu\text{l)} &= \text{WBC count}^{CD} \times \%\ \text{of Lin1}^-\text{HLA-DR}^+ \\ &CD123^+\text{or Lin1}^-\text{HLA-DR}^+CD11c^{+FM}\end{aligned}$$

(where CD indicates the clinical data and FM indicates the flow cytometry data).

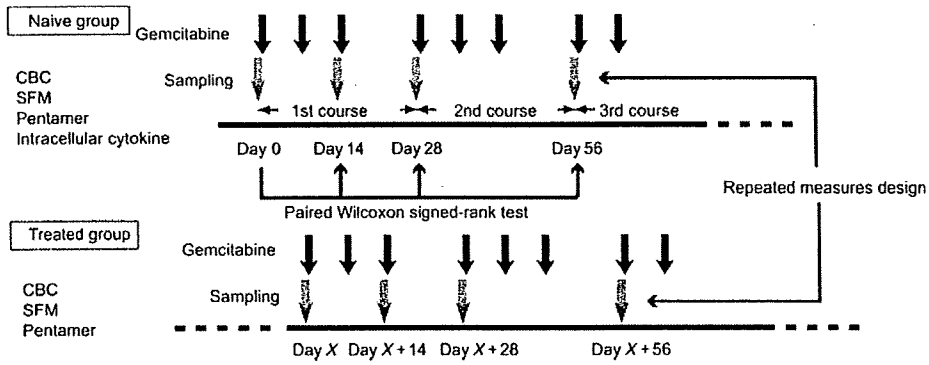

Figure 1. Schedules of gemcitabine treatment (brack arrows) and blood sampling (gray arrows), with a schematic of the analysis. Two cohorts (the naive group and the treated group) were examined in this study to confirm the long-term immunological effect of gemcitabine. CBC, complete blood count; SFM, surface maker staining (cell phenotype).

Table 1. The panel of fluorescent-conjugated monoclonal antibodies

No.	FITC	PE	PerCP	Analysis	Short names
1	IgG1[a]	IgG1[a]	IgG1[a]	$IgG1^+IgG1^+IgG1^-$	Negative control
2	CD4-FITC/CD8-PE[b]		CD3[a]	$CD4^-CD8^-CD3^+$	$CD4^+$ T cell
				$CD4^-CD8^+CD3^+$	$CD8^+$ T cell
3	CD16[a]	CD56[a]	CD3[a]	$CD16^+CD56^+CD3^-$	NK cell
4	Vα24[a]	CD161[a]	CD3[a]	$Vα24^-CD161^+CD3^+$	NKT cell
5	CD14[a]	CD20[a]		$CD14^+CD20^-$	$CD14^+$ monocyte
				$CD14^-CD20^+$	B cell
6	CD45RA[b]	CD45RO[b]	CD4[a]	$CD45RA^+CD45RO^-CD4^+$	Naive $CD4^+$ lymphocyte
				$CD45RA^-CD45RO^+CD4^+$	Memory $CD8^+$ lymphocyte
7	CD3[a]	CD69[a]	CD4[a]	$CD3^-CD69^+CD4^-$	$CD69^+CD4^+$ T cell
8	CD3[a]	CD69[a]	CD8[a]	$CD3^-CD69^+CD8^-$	$CD69^+CD8^+$ T cell
9	CD3[a]	CD25[a]	CD4[a]	$CD3^-CD25^+CD4^-$	$CD4^+CD25^+$ T cell
10	GITR[c]	CD25[a]	CD4[a]	$GITR^+CD25^+CD4^+$	
11	Lin-1[a]	CD123[a]	Anti-HLA-DR[a]	$Lin\text{-}1^-CD123^+HLA\text{-}DR^+$	$CD123^+$ dendritic cell
12	Lin-1[a]	CD11c[a]	Anti-HLA-DR[a]	$Lin\text{-}1^-CD11c^+HLA\text{-}DR^+$	$CD11c^-$ dendritic cell

Vα24, TCR Vα24; GITR, TNF receptor family-related; Lin-1, Lineage Cocktail 1.
[a]BD Biosciences, San Diego, CA, USA.
[b]Beckman–Coulter, Fullerton, CA, USA.
[c]R&D Systems, Minneapolis, MN, USA.

HLA Analysis

Before antigen-specific T cells were analyzed with regard to human leukocyte antigen (HLA)-pentamer and intracellular cytokine production, HLA typing was performed. Samples were stained with HLA-A02-FITC and HLA-A24-PE (BD) and analyzed by flow cytometry. Only HLA-A02 and -A24 patients were enrolled in the antigen-specific T cell analysis.

Pentamer Staining

Complexes of HLA-0201 CMV peptide (NLVPMVATV), WT1 peptide (RMFPNAPYL) and HLA-2402 WT1 peptide (CMTWNQMNL) were purchased from PROIMMUNE (Oxford, UK). Patients with HLA-A02 were examined for CMV and WT1, and patients with HLA-A24 were examined for WT1-specific TCR. CD3-FITC, CCR7-PE, CD3-PerCP and APC-conjugated pentamer were added to whole blood and incubated for 15 min at room temperature in the dark. The red blood cells were then lysed twice after antibody staining. After being washed with washing buffer, the cells were fixed and acquired on a flow cytometer. If there were enough pentamer-positive cells, we also performed CD45RA-FITC (Beckman–Coulter), CD57-FITC (BD), CD45RO-PE (Beckman–Coulter), CD27-PE (BD), CD8-PerCP and Pentamer-APC staining.

Peptides and CMV Lysate

The following >80% pure peptides, which were assessed as WT1 antigen epitope, were obtained using high-performance liquid chromatography (Qiagen, Hilden, Germany). The sequence of HLA-A0201-binding WT1 peptide was RMFPNAPYL [amino acids (AA) 126–134] and that of HLA-A2402-binding WT1 peptide was CMTWNQMNL (AA 235–243). CMV AD169 viral lysate was purchased from Advanced Biotechnologies (Alberta, Canada).

Intracellular Cytokine Staining

Intracellular cytokine staining was performed only in the naive group. Peripheral whole blood (1 ml) was stimulated for 6 h at 37°C with 1.0 μg/ml CMV lysate in the presence of 10 μg/ml co-stimulatory MAbs, CD28 and CD49d (BD). Patients with HLA-A02 or -A24 also received specific WT1-peptide stimulation at a final concentration of 1 ng/ml. 10 μg/ml breferdin A (Sigma, St Louis, MO, USA) was added during the last 4 h of incubation. Positive and negative controls were obtained by stimulating cells with 5 μl/ml staphylococcal enterotoxin B (Sigma) as a positive control or PBS (Ca^{2+}–Mg^{2+}) as a negative control. Samples were lysed by Lysing solution (BD), permeabilized by Permealyzing solution (BD) and stained with CD69-FITC, IL-4-PE, IFN-γ -PE, CD8-PerCP, CD4-PerCP and CD3-APC

(BD), before analysis with a FACSCalibur. Intracellular interferon (IFN)-γ- or interleukin (IL)-4-positive cells in $CD3^+CD4^+$ or $CD3^+CD8^+$ cells in lymphocyte gate were defined as cytokine-secreting T cells. CD69 was used as a marker for T cell activation.

T Cell Repertoire Analysis

Five samples were analyzed. Three milliliters of whole blood with EDTA were used for RNA extraction. RNA was extracted by a QIAamp RNA Blood Mini Kit (Qiagen), and an RT–PCR and PCR amplification were performed with a TaKaRa One Step RNA PCR Kit (AMV) (TaKaRa BIO Inc., Shiga, Japan) according to the supplier's protocol. The PCR conditions were: one cycle of 50°C for 30 min and 94°C for 2 min, followed by 30 cycles of 94°C for 30 s, 57°C for 30 s and 72°C for 30 s, with a final 1 min extension at 72°C and holding at 4°C (GeneAmp PCR System 9700, Applied Biosystems, CA, USA). We used 26 kinds of TCR-Vβ chain as forward primers with a Cβchain-conjugated 6FAM as a reverse primer (10,11). Vβ primers were synthesized by Invitrogen (CA, USA) and Cβ primer was synthesized by Applied Biosystems. One microliter of PCR product was mixed with 13.6 μl formamide and 0.4 μl size standard (Genescan-500 ROX, ABI), denatured at 94°C for 5 min and electrophoresed with a 3100-Avant Genetic Analyzer (ABI). The distribution was analyzed with GeneScan 7.7 (ABI).

Statistical Analysis

Progression-free survival was measured from the first day of gemcitabine treatment until the diagnosis of progressive disease, and data were analyzed by the Kaplan–Meier method. The log-rank test was used to analyze the differences between groups. Figure 1 shows a schematic of the analysis. In the naive group, we compared the immunological status pre-treatment to that after treatment by a paired Wilcoxon signed rank test. To compare the immunological status of the naive and treated groups, a repeated measures design was used. Data were analyzed with JMP 6.0 for Windows.

RESULTS

Patients

Twenty-eight patients were enrolled into this study (Table 2). Eighteen patients were receiving their first treatment with gemcitabine (naive group) and 10 had already received 3–20 previous courses of gemcitabine (treated group). In the naive group, three patients discontinued treatment due to early progression, pneumonia and entered the best supportive care, respectively. Five patients in the naive group and three in the treated group changed their schedule because they felt bad, showed fever associated with a common cold, had acute pancreatitis, showed stent obstruction and private matters. The patient data obtained during fever, pancreatitis and stent obstructions were removed from the analysis due to the suspension of gemcitabine treatment.

White Blood Cell Count, Neutrophils, Lymphocytes and Monocytes

We evaluated the white blood cell count (WBC), including a differential analysis of neutrophils, lymphocytes and monocytes (Fig. 2A–C and Supplementary Fig. S1A–C). The solid and dotted lines indicate the median number of cells in the naive and treated groups individually. The monocyte count in the naive group was lower than that in the treated group in a repeated measures analysis ($P = 0.001$). However, during the first 2 months, the number of monocytes increased significantly compared with the pre-treatment value at the beginning of the third course in the naive group ($P = 0.025$). Two months of gemcitabine treatment led to an increase in monocytes in the naive group to the same level as that in the treated group (Fig. 2C). The decrease in the lymphocyte count during the treatment course was transient, and only 5.6% of the patients in the naive group showed Grade 3–4 lymphopenia. Our data suggested that lymphocytes were not significantly influenced by gemcitabine treatment (Fig. 2B). There were no differences in the numbers of WBC, neutrophils, lymphocytes and monocytes between days 7 and 14, which suggested that these cells decreased by day 7 when the cell kinetics became stable.

Surface Markers

The counts of $CD69^+CD4^+$ T cells ($P = 0.002$), $CD69^+CD8^+$ T cells ($P = 0.012$) and $CD14^+$ monocytes ($P = 0.021$) (Fig. 2L, M and I), and two types of DC, $CD123^+$ and $CD11c^+$ ($P < 0.001$ and $P < 0.001$, Fig. 2P and Q) significantly increased in the treated group by a repeated measures analysis. The percentage of NK cells significantly decreased ($P = 0.008$) in the treated group (Supplementary Fig. S1F), but the absolute number was not significantly different ($P = 0.072$). Nevertheless, the tendency for the decrease in the treated group was clear (Fig. 2F). None of the other lymphocyte subtypes changed with regard to either number or percentage in the two groups. In comparison with pre-treatment and post-treatment in the naive group, the percentages of $CD4^+$ T cells ($P = 0.008$) and naive $CD4^+$ lymphocytes ($P < 0.001$) increased on day 14 (Supplementary Fig. S1D and J), whereas no significant change was observed in the other lymphocytes. In DC, the percentage of $CD123^+$ DC increased from the beginning of the second course ($P = 0.003$) and $CD11c^+$ DC increased from day 14 in the first course ($P < 0.001$) (Supplementary Fig. S1P and Q). The absolute numbers of most immune cells decreased. NK cells ($P = 0.018$)

Table 2. Patients' characteristics

No.	Group (courses of treatments)	Age	Sex	KPS	Stage (metastasis)	Comment
1	Naive	50	M	90	Locally advanced	The third injection of the first course was omitted by high fever
2	Naive	57	M	90	Locally advanced	
3	Treated (3)	74	F	100	Locally advanced	The third course was irregular by patient's private matter
4	Treated (4)	76	M	90	Locally advanced	The second course was irregular by pancreatitis
5	Treated (20)	70	F	90	Metastasis (HEP)	
6	Treated (9)	56	M	100	Locally advanced	The second injection of the second course was omitted by high fever
7	Naive	62	F	90	Metastasis (HEP, SPL)	
8	Naive	81	M	90	Locally advanced	
9	Treated (3)	68	F	90	Locally advanced	
10	Treated (5)	70	M	100	Locally advanced	
11	Naive	74	F	100	Metastasis (PUL)	The third course was irregular by nausea
12	Treated (12)	72	M	100	Metastasis (PER)	
13	Treated (9)	54	F	100	Metastasis (HEP)	
14	Naive	70	M	100	Metastasis (PUL, PLE)	Terminated by PD in the second course
15	Naive	57	F	80	Metastasis (PLE, OSS)	Terminated by pneumonia in the first course
16	Treated (8)	64	M	90	Locally advanced	
17	Treated (5)	78	F	90	Metastasis (PER)	
18	Naive	56	F	90	Locally advanced	
19	Naive	48	M	90	Locally advanced	
20	Naive	80	M	100	Locally advanced	
21	Naive	59	F	80	Metastasis (HEP)	Terminated by PD in the second course
22	Naive	65	F	90	Locally advanced	The second injection of the second course was omitted by high fever
23	Naive	52	M	90	Locally advanced	The first course was irregular by neutropenia
24	Naive	78	F	90	Locally advanced	
25	Naive	65	F	100	Metastasis (HEP)	
26	Naive	80	F	100	Metastasis (LN)	
27	Naive	82	F	100	Metastasis (PER, LN)	
28	Naive	71	F	90	Metastasis (PUL)	The second injection of the second course was omitted by patient's private matter

KPS, Karnofsky performance score; HEP, liver; SPL, spleen; PUL, lung; PER, peritoneum; PLE, pleura; OSS, bone; LN, lymph node; PD, progressive disease.

(Fig. 2F), $CD69^+CD4^+$ T cells ($P = 0.048$) (Fig. 2L) and $CD69^+CD8^+$ T cells ($P = 0.015$) (Fig. 2M) decreased on day 14. $CD8^+$ T cells ($P = 0.010$ and $P = 0.030$) and memory CD4 lymphocytes ($P = 0.020$ and $P = 0.010$) took 2 months to recover (Fig. 2E and K). B cells ($P = 0.022$, $P = 0.011$ and $P = 0.005$, Fig. 2H) and NKT cells ($P = 0.035$, $P = 0.042$ and $P = 0.013$, Fig. 2G) did not recover during the 2 months of the monitoring period. $CD123^+$ DC increased before the second course ($P = 0.017$), and there was no significant difference between the third course (Fig. 2P). Only $CD11c^+$ DC showed a constant increase over 2 months ($P = 0.011$ and $P = 0.021$, Fig. 2Q). $CD14^+$ monocytes temporarily decreased at day 14, but returned to the pre-treatment count before the third course of treatment ($P = 0.033$, Fig. 2I).

Pentamer Analysis

The percentage of CMV-specific T cell was examined in seven patients in the naive group and four in the treated group (Supplementary Fig. S2). The percentage of CMV-positive cells was not different between the naive and treated groups (Supplementary Fig. S2A). A subtype analysis was performed in Patient no. 27 and there were no changes in the percentages of naive ($CD8^+CD27^+CD45RA^+$), memory ($CD8^+CD45RA^-$), effector ($CD8^+CD27^-CD45RA^+$) and central memory cells ($CD8^+CD57^-CD45RO^+$) (Supplementary Fig. S2B). Hence, gemcitabine treatment did not affect CMV-specific T cells. WT1-specific T cells were examined by a pentamer analysis in 5 patients with HLA-A02, 10 patients with HLA-A24 and

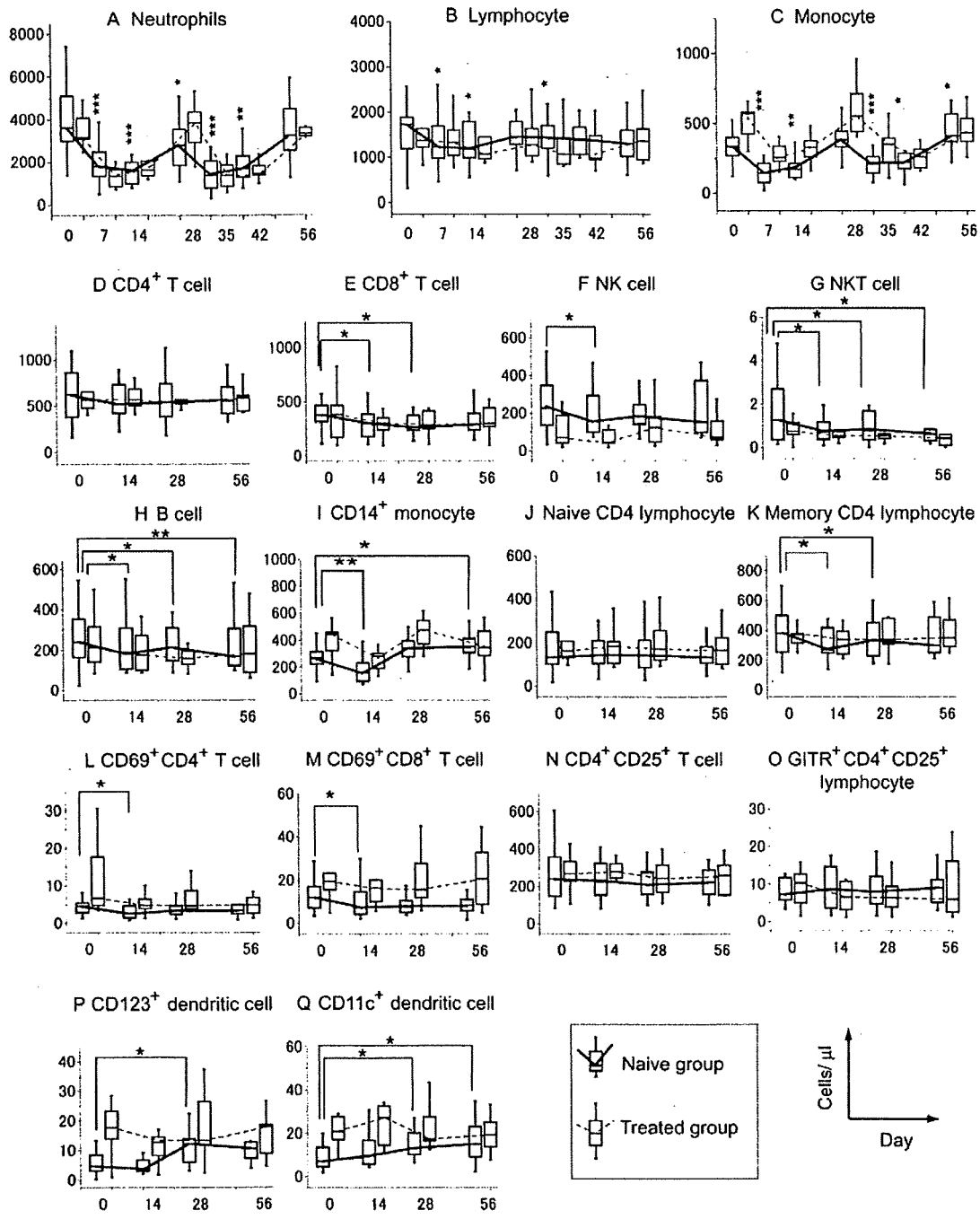

Figure 2. Kinetic of absolute numbers of immune cells during gemcitabine treatment. $CD69^+CD4^+$ T cell (L), D69 $CD8^+$ T cell (M), $CD14^+$ monocyte (I), $CD123^+$ dendritic cell (P) and $CD11c^+$ dendritic cell (Q) increased in the treated group. $CD14^+$ monocyte (I), $CD123^-$ dendritic cell (P) and $CD11c^+$ dendritic cell (Q) increased gradually, following gemcitabine treatment in the naive group. Significant difference between pre-treatment and post-treatment samples in the naive group: *, ** and *** indicates $P < 0.050$, $P < 0.010$ and $P < 0.001$, respectively. P value of the naive group vs. the treated group by repeated measured design. A, $P = 0.444$; B, $P = 0.753$; C, $P = 0.001$; D, $P = 0.572$; E, $P = 0.791$; F, $P = 0.072$; G, $P = 0.166$; H, $P = 0.099$; I, $P = 0.021$; J, $P = 0.663$; K, $P = 0.838$; L, $P = 0.002$; M, $P = 0.012$; N, $P = 0.551$; O, $P = 0.433$; P, $P < 0.001$; Q, $P < 0.001$.

6 patients with HLA-A02/A24 (Supplementary Fig. S2C). The frequency of WT1 pentamer-positive cells in HLA-A24 cells tended to be higher than that in HLA-A02. However, HLA-A2402 WT1 pentamer-positive cells did not make cluster patterns and were considered as non-specific binding.

Intracellular Cytokine Analysis and T Cell Repertoire Analysis

The absolute numbers and percentages of IL-4- and IFN-γ-producing T cells in $CD8^+$ and $CD4^+$ T cells were analyzed (Fig. 3 and Supplementary Fig. S3). Gemcitabine

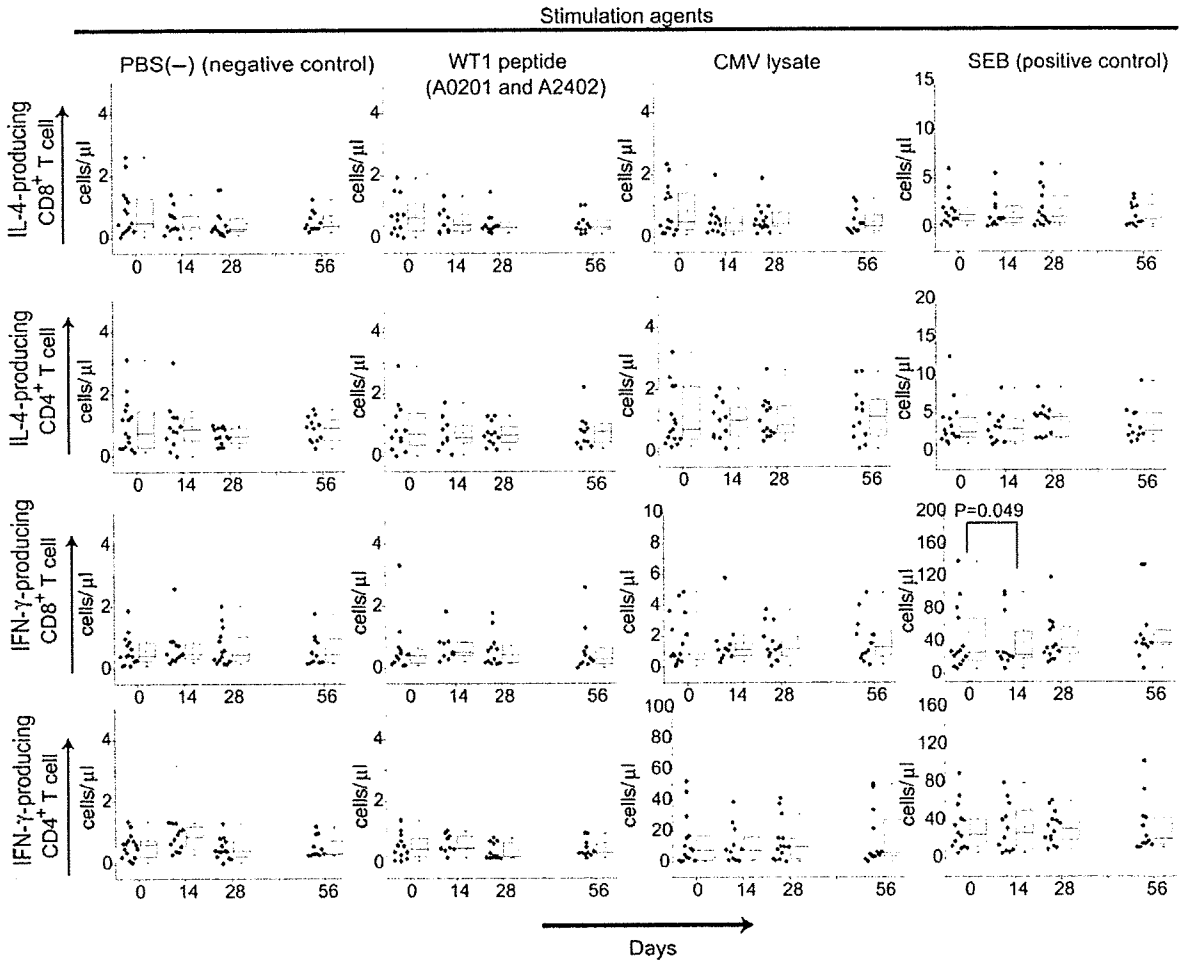

Figure 3. Kinetic of the absolute number of cytokine-producing cells during gemcitabine treatment. Cytokine production stimulated with WT1 peptides, CMV lysate or SEB was not influenced by gemcitabine treatment, except for interferon (IFN)-γ production of $CD8^+$ T cell stimulated with SEB.

treatment only influenced the absolute number of IFN-γ-producing $CD3^+CD8^+$ lymphocytes as determined by staphylococcal enterotoxin B (SEB) stimulation (on day 14, $P = 0.049$). The level of cytokine production inducted by WT1-peptide stimulation was same as PBS(−) (negative control). A simple regression analysis revealed a strong correlation between them ($R = 0.66799–0.88675$) and suggested that compensation by subtracting the percentage of negative control is needed to detect actual reactivation with WT1 peptide. Figure 4 shows the compensated percentage of cytokine-producing cells. The compensated percentage of IL-4- and IFN-γ-producing cells induced by WT1-peptide stimulation was <0.3%, suggesting that WT1 peptides had almost no effects for cytokine production in this study. The difference in percentage of IL-4-producing cells induced by CMV lysate or SEB was statistically significant between pre-treatment and post-treatment; however, the change of the percentage was very small and considered to be of little importance.

T cell repertoire analysis was performed in five patients in the naive group. The size distribution of TCR did not show any significant change which suggests that gemcitabine does not affect the T cell repertoire.

DISCUSSION

As our knowledge of cellular and molecular immunology has increased, the mechanism of anticancer immunity has been explored and many tumor-associated antigens have been identified, which has contributed to the recent development of cancer vaccine trials. Although prophylactic cancer vaccine against cervical cancers (GARDASIL®, CERVARIX®) has already been approved in several countries, clinical trials of therapeutic cancer vaccines have shown only limited efficacy (12). To improve the efficacy of therapeutic cancer vaccines, several approaches have been tried. One strategy is to give such vaccines to patients with minimal residual disease (13), and another is to give vaccines in combination with chemotherapeutic agents and/or radiotherapy to temporarily control cancer growth and/or to

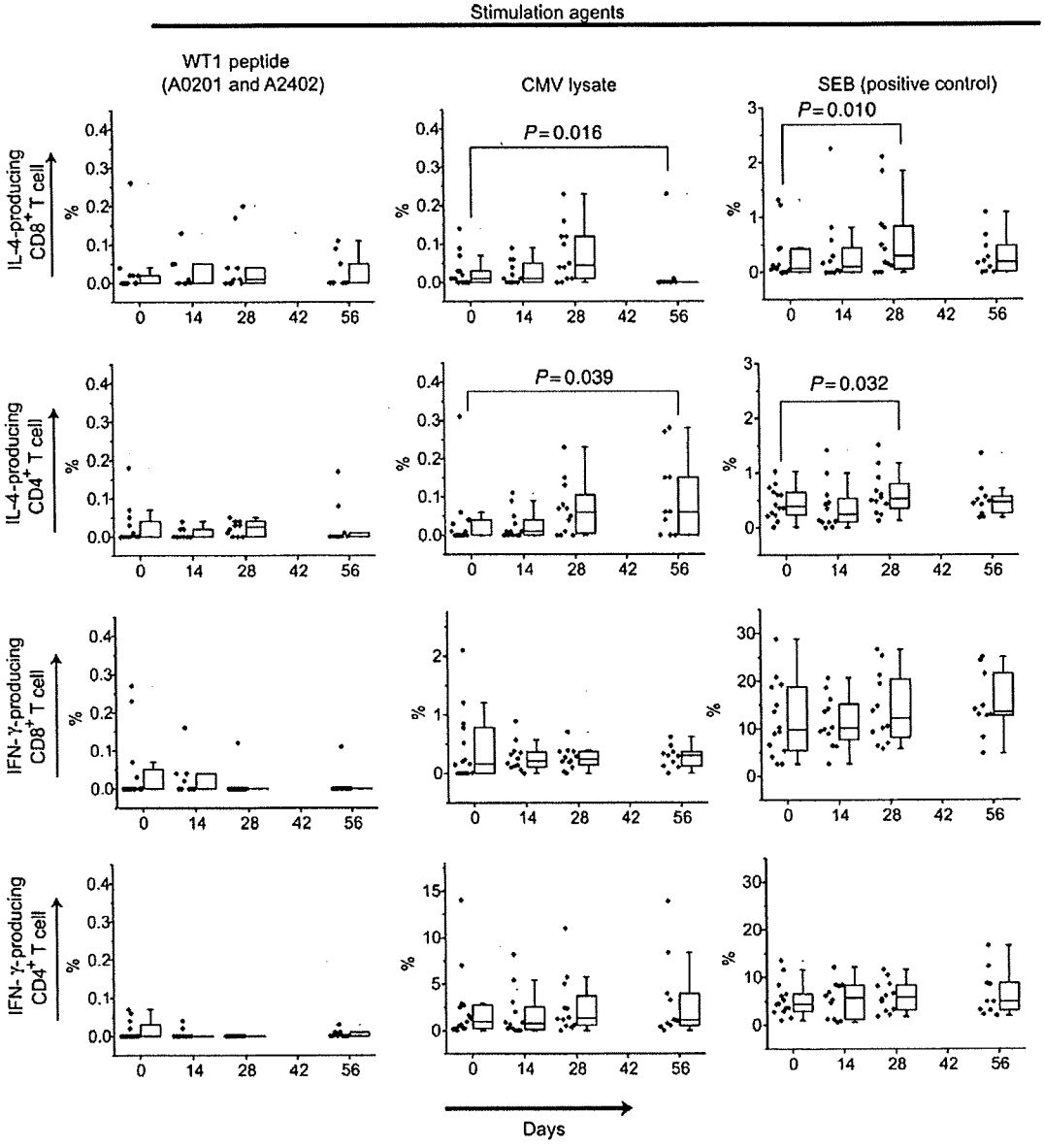

Figure 4. The compensated percentage of cytokine-producing cells in each T cell subtype. The percentage of interleukin (IL)-4- and IFN-γ-producing cells was <0.3% by WT1-peptide stimulation. The difference in IL-4 production stimulated by CMV lysate and SEB was statistically significant; however, the change was very small.

achieve synergistic effects (14,15). It is well known that many cytotoxic drugs induce an immunosuppressive status and some of them are actually used as immunosuppressants for the treatment of autoimmune diseases and as post-transplantation prophylaxis for graft-versus-host disease. On the other hand, it was recently revealed that some chemotherapeutic agents induce positive immunological reactions. Cyclophosphamide enhanced anti-tumor immunity by reducing the immunosuppressive effects of $CD4^+CD25^+$ regulatory T cells (16). Oxaliplatin and doxorubicin also enhance immunity by injuring tumor cells to release HMGB1 protein, which is a ligand of Toll-like receptor-4 that activates DC (17). Cytotoxic agents including cisplatin, doxorubicin, mitomycin C, fluorouracil and camptothecin induce the apoptosis of cancer cells via Fas or TRAIL-dependent pathways (18,19).

Gemcitabine has multiple immunostimulatory effects. It enhances antigen presentation by inducing tumor apoptosis (20,21) and eliminates myeloid-derived suppressor cells (22). It was also reported that gemcitabine treatment inhibited B-cell proliferation and the production of anti-influenza virus antibody in a mouse model (23). Nowak et al. (24) reported that gemcitabine and CD40L had synergistic effects toward solid tumors. Bauer et al. (25) also showed that combination therapy with gemcitabine and DC-based vaccination had higher efficacy in a Panc02 pancreatic tumor cell line.

Furthermore, Correale et al. (26) reported the results of a clinical trial of chemo-immunotherapy against colon cancer with gemcitabine plus FOLFOX4 followed by granulocyte-macrophage colony-stimulating factor and IL-2. They showed an increase in the expression of tumor-associated antigen (carcinoembryonic antigen and thymidylate synthase) and a suppression of regulatory T cells. However, the mechanism by which gemcitabine affects the immune system is not yet fully elucidated. The results of immunological monitoring in pancreatic cancer patients were reported by Plate et al. (9) who concluded that gemcitabine therapy was not immunosuppressive and may actually enhance the response to vaccine by reducing $CD3^+CD45RO^+$ memory T cells. However, their study encompassed a shorter period of only 21 days, and the gemcitabine treatment schedule was different from ours. Bang et al. (27) reported an increase in $CD11c^+$ myeloid DC under combination therapy with gemcitabine and cisplatin.

In this study, we evaluated the immunological effects of gemcitabine as a single agent over a 2-month period in pancreatic cancer patients. Our results showed that the decreases in T lymphocytes and NK cells were transient, and gemcitabine treatment increased CD14+ monocytes and two types of DC. We showed that conventional gemcitabine treatment increased the number of antigen-presenting cells (APCs). In cancer patients, it has been reported that levels of circulating DC were lower than those in healthy individuals (28) and the differentiation of DC was inhibited by tumor cells (29,30). Our result indicated that gemcitabine may act on APC both locally and systemically in a clinical setting. This reaction may activate innate immunity and then stimulate the acquired immune system via activated APC, and finally induce tumor cell death. These effects of gemcitabine on APCs may be an advantage of combination therapy with cancer vaccine.

Previously, we reported that the appearance of WT1-specific T lymphocytes after allogeneic hematopoietic stem cell transplantation correlated with the development of graft-versus-host disease and the clinical response for malignant diseases (31). WT1 protein is found in leukemia (32), breast cancer (33) and many solid cancer cell lines (34), and clinical trials of WT1-peptide vaccine have already been started by several groups (35,36). Pancreatic cancer also expresses WT1 protein in 75% of the cases (37). Antigen-specific T cells and IFN-producing function were not affected by gemcitabine treatment. All of these results suggest that the combination of gemcitabine and WT1-peptide vaccine could be a suitable chemo-immunotherapy against pancreatic cancers.

Our study also demonstrated several limitations to establish the proof of concept in our future WT1-peptide therapy. In WT1-specific pentamer analysis, the specificity of HLA-A0201-restricted pentamer appears to be a useful tool for evaluating WT1-specific cytotoxic T lymphocyte. However, HLA-A2402 pentamer showed non-specific binding potential to CD8-negative T lymphocytes, which results in a wide distribution of CD8-positive/negative cells. None of the samples clearly secreted INF-γ after HLA-A2402 peptide stimulation, even if they contained pentamer-positive cells. Even though the patients in the gemcitabine naive and treated groups had almost the same backgrounds, several patients in the naive group discontinued gemcitabine treatment, which suggests that the two groups actually reflect different populations. Indeed, progression-free survival in the naive and treated groups was 6 vs. 20.6 months ($P < 0.001$). Nevertheless, our results may still suggest that combination therapy consisting of gemcitabine and WT1-peptide vaccine may become a novel chemo-immunotherapy against advanced pancreatic cancer.

Supplementary data

Supplementary data are available at http://www.jjco.oxfordjournals.org.

Funding

This study was supported by Grants in Aid for Cancer Research from Ministry of Health, Labour and Welfare of Japan.

Conflict of interest statement

None declared.

References

1. Ministry of Health, Labour and Welfare. Abridged Life Table for Japan 2006. http://www.mhlw.go.jp/toukei/saikin/hw/jinkou/kakutei06/hyo7.html (1 December 2008, date last accessed).
2. Jemal A, Siegel R, Ward E, Murray T, Xu J, Thun MJ. Cancer statistics. *CA Cancer J Clin* 2007;57:43–66.
3. Burris HA, Moore MJ, Andersen J, Green MR, Rothenberg ML, Modiano MR, et al. Improvements in survival and clinical benefit with gemcitabine as first-line therapy for patients with advanced pancreas cancer: a randomized trial. *J Clin Oncol* 1997;15:2403–13.
4. Berlin JD, Catalano P, Thomas JP, Kugler JW, Haller DG, Benson AB. Phase III study of gemcitabine in combination with fluorouracil versus gemcitabine alone in patients with advanced pancreatic carcinoma: Eastern Cooperative Oncology Group Trial E2297. *J Clin Oncol* 2002;20:3270–5.
5. Louvet C, Labianca R, Hammel P, Lledo G, Zampino MG, Andre T, et al. Gemcitabine in combination with oxaliplatin compared with gemcitabine alone in locally advanced or metastatic pancreatic cancer: results of a GERCOR and GISCAD phase III trial. *J Clin Oncol* 2005;23:3509–16.
6. Oettle H, Richards D, Ramanathan RK, van Laethem JL, Peeters M, Fuchs M, et al. A phase III trial of pemetrexed plus gemcitabine versus gemcitabine in patients with unresectable or metastatic pancreatic cancer. *Ann Oncol* 2005;16:1639–45.
7. Van Cutsem E, van de Velde H, Karasek P, Oettle H, Vervenne WL, Szawlowski A, et al. Phase III trial of gemcitabine plus tipifarnib compared with gemcitabine plus placebo in advanced pancreatic cancer. *J Clin Oncol* 2004;22:1430–8.
8. Moore MJ, Goldstein D, Hamm J, Figer A, Hecht JR, Gallinger S, et al. Erlotinib plus gemcitabine compared with gemcitabine alone in patients with advanced pancreatic cancer: a phase III trial of the National

Cancer Institute of Canada Clinical Trials Group. *J Clin Oncol* 2007;25:1960–6.
9. Plate JM, Plate AE, Shott S, Bograd S, Harris JE. Effect of gemcitabine on immune cells in subjects with adenocarcinoma of the pancreas. *Cancer Immunol Immunother* 2005;54:915–25.
10. Choi YW, Kotzin B, Herron L, Callahan J, Marrack P, Kappler J. Interaction of *Staphylococcus aureus* toxin 'superantigens' with human T cells. *Proc Natl Acad Sci USA* 1989;86:8941–5.
11. Labrecque N, McGrath H, Subramanyam M, Huber BT, Sekaly RP. Human T cells respond to mouse mammary tumor virus-encoded superantigen: V beta restriction and conserved evolutionary features. *J Exp Med* 1993;177:1735–43.
12. Rosenberg SA, Yang JC, Restifo NP. Cancer immunotherapy: moving beyond current vaccines. *Nat Med* 2004;10:909–15.
13. Hoos A, Parmiani G, Hege K. A clinical development paradigm for cancer vaccines and related biologics. *J Immunother* 2007;30:1–15.
14. Menard C, Martin F, Apetoh L, Bouyer F, Ghiringhelli F. Cancer chemotherapy: not only a direct cytotoxic effect, but also an adjuvant for antitumor immunity. *Cancer Immunol Immunother* 2008;57: 1579–87.
15. Zitvogel L, Apetoh L, Ghiringhelli F, Kroemer G. Immunological aspects of cancer chemotherapy. *Nat Rev Immunol* 2008;8:59–73.
16. Ghiringhelli F, Menard C, Puig PE, Ladoire S, Roux S, Martin F, et al. Metronomic cyclophosphamide regimen selectively depletes $CD4^+CD25^+$ regulatory T cells and restores T and NK effector functions in end stage cancer patients. *Cancer Immunol Immunother* 2007;56:641–8.
17. Apetoh L, Ghiringhelli F, Tesniere A, Obeid M, Ortiz C, Criollo A, et al. Toll-like receptor 4-dependent contribution of the immune system to anticancer chemotherapy and radiotherapy. *Nat Med* 2007;13: 1050–9.
18. Lacour S, Hammann A, Wotawa A, Corcos L, Solary E, Dimanche-Boitrel MT. Anticancer agents sensitize tumor cells to tumor necrosis factor-related apoptosis-inducing ligand-mediated caspase-8 activation and apoptosis. *Cancer Res* 2001;61:1645–51.
19. Micheau O, Solary E, Hammann A, Martin F, Dimanche-Boitrel MT. Sensitization of cancer cells treated with cytotoxic drugs to fas-mediated cytotoxicity. *J Natl Cancer Inst* 1997;89:783–9.
20. Zisman A, Ng CP, Pantuck AJ, Bonavida B, Belldegrun AS. Actinomycin D and gemcitabine synergistically sensitize androgen-independent prostate cancer cells to Apo2L/TRAIL-mediated apoptosis. *J Immunother* 2001;24:459–71.
21. Correale P, Cusi MG, Del Vecchio MT, Aquino A, Prete SP, Tsang KY, et al. Dendritic cell-mediated cross-presentation of antigens derived from colon carcinoma cells exposed to a highly cytotoxic multidrug regimen with gemcitabine, oxaliplatin, 5-fluorouracil, and leucovorin, elicits a powerful human antigen-specific CTL response with antitumor activity in vitro. *J Immunol* 2005;175:820–8.
22. Suzuki E, Kapoor V, Jassar AS, Kaiser LR, Albelda SM. Gemcitabine selectively eliminates splenic Gr-1+/CD11b+ myeloid suppressor cells in tumor-bearing animals and enhances antitumor immune activity. *Clin Cancer Res* 2005;11:6713–21.
23. Nowak AK, Robinson BW, Lake RA. Gemcitabine exerts a selective effect on the humoral immune response: implications for combination chemo-immunotherapy. *Cancer Res* 2002;62:2353–58.
24. Nowak AK, Robinson BW, Lake RA. Synergy between chemotherapy and immunotherapy in the treatment of established murine solid tumors. *Cancer Res* 2003;63:4490–6.
25. Bauer CA, Bauernfeind F, Sterzik A, Orban M, Schnurr M, Lehr HA, et al. Dendritic cell-based vaccination combined with gemcitabine increases survival in a murine pancreatic carcinoma model. *Gut* 2007;56:1275–82.
26. Correale P, Cusi MG, Tsang KY, Del Vecchio MT, Marsili S, Placa ML, et al. Chemo-immunotherapy of metastatic colorectal carcinoma with gemcitabine plus FOLFOX 4 followed by subcutaneous granulocyte macrophage colony-stimulating factor and interleukin-2 induces strong immunologic and antitumor activity in metastatic colon cancer patients. *J Clin Oncol* 2005;23:8950–8.
27. Bang S, Kim HS, Choo YS, Park SW, Chung JB, Song SY. Differences in immune cells engaged in cell-mediated immunity after chemotherapy for far advanced pancreatic cancer. *Pancreas* 2006;32:29–36.
28. Almand B, Resser JR, Lindman B, Nadaf S, Clark JI, Kwon ED, et al. Clinical significance of defective dendritic cell differentiation in cancer. *Clin Cancer Res* 2000;6:1755–66.
29. Oyama T, Ran S, Ishida T, Nadaf S, Kerr L, Carbone DP, et al. Vascular endothelial growth factor affects dendritic cell maturation through the inhibition of nuclear factor-kappa B activation in hemopoietic progenitor cells. *J Immunol* 1998;160:1224–32.
30. Gabrilovich DI, Chen HL, Girgis KR, Cunningham HT, Meny GM, Nadaf S, et al. Production of vascular endothelial growth factor by human tumors inhibits the functional maturation of dendritic cells. *Nat Med* 1996;2:1096–103.
31. Morita Y, Heike Y, Kawakami M, Miura O, Nakatsuka S, Ebisawa M, et al. Monitoring of WT1-specific cytotoxic T lymphocytes after allogeneic hematopoietic stem cell transplantation. *Int J Cancer* 2006;119:1360–7.
32. Inoue K, Sugiyama H, Ogawa H, Nakagawa M, Yamagami T, Miwa H, et al. WT1 as a new prognostic factor and a new marker for the detection of minimal residual disease in acute leukemia. *Blood* 1994;84:3071–9.
33. Loeb DM, Evron E, Patel CB, Sharma PM, Niranjan B, Buluwela L, et al. Wilms' tumor suppressor gene (WT1) is expressed in primary breast tumors despite tumor-specific promoter methylation. *Cancer Res* 2001;61:921–5.
34. Oji Y, Ogawa H, Tamaki H, Oka Y, Tsuboi A, Kim EH, et al. Expression of the Wilms' tumor gene WT1 in solid tumors and its involvement in tumor cell growth. *Jpn J Cancer Res* 1999;90:194–204.
35. Morita S, Oka Y, Tsuboi A, Kawakami M, Maruno M, Izumoto S, et al. A phase I/II trial of a WT1 (Wilms' tumor gene) peptide vaccine in patients with solid malignancy: safety assessment based on the phase I data. *Jpn J Clin Oncol* 2006;36:231–6.
36. Oka Y, Tsuboi A, Taguchi T, Osaki T, Kyo T, Nakajima H, et al. Induction of WT1 (Wilms' tumor gene)-specific cytotoxic T lymphocytes by WT1 peptide vaccine and the resultant cancer regression. *Proc Natl Acad Sci USA* 2004;101:13885–90.
37. Oji Y, Nakamori S, Fujikawa M, Nakatsuka S, Yokota A, Tatsumi N, et al. Overexpression of the Wilms' tumor gene WT1 in pancreatic ductal adenocarcinoma. *Cancer Sci* 2004;95:583–7.

The Pharmacogenomics Journal (2009) 9, 137–146
© 2009 Nature Publishing Group All rights reserved 1470-269X/09 $32.00
www.nature.com/tpj

ORIGINAL ARTICLE

A new statistical screening approach for finding pharmacokinetics-related genes in genome-wide studies

Y Sato[1,2], NM Laird[1], K Nagashima[3], R Kato[3], T Hamano[4], A Yafune[5], N Kaniwa[6,7], Y Saito[6,8], E Sugiyama[6,7], S-R Kim[6], J Furuse[9], H Ishii[9], H Ueno[10], T Okusaka[10], N Saijo[11], J-i Sawada[6,8] and T Yoshida[2]

[1]*Department of Biostatistics, Harvard School of Public Health, Boston, MA, USA;* [2]*Genetics Division, National Cancer Center Research Institute, Tokyo, Japan;* [3]*Faculty of Engineering, Tokyo University of Science, Tokyo, Japan;* [4]*Hamano Statistical Analysis Ltd., Tokyo, Japan;* [5]*Clinic Sendagaya, Tokyo, Japan;* [6]*Project Team for Pharmacogenetics, National Institute of Health Sciences, Tokyo, Japan;* [7]*Division of Medicinal Safety Science, National Institute of Health Sciences, Tokyo, Japan;* [8]*Division of Functional Biochemistry and Genomics, National Institute of Health Sciences, Tokyo, Japan;* [9]*Hepatobiliary and Pancreatic Oncology Division, National Cancer Center Hospital East, Chiba, Japan;* [10]*Hepatobiliary and Pancreatic Oncology Division, National Cancer Center Hospital, Tokyo, Japan and* [11]*National Cancer Center Hospital East, Chiba, Japan*

Correspondence:
Dr T Yoshida, Genetics Division, National Cancer Center Research Institute, 5-1-1 Tsukiji, Chuo-ku, Tokyo 104-0045, Japan.
E-mail: tyoshida@ncc.go.jp

Received 7 August 2008; revised 11 November 2008; accepted 19 November 2008; published online 23 December 2008

Biomedical researchers usually test the null hypothesis that there is no difference of the population mean of pharmacokinetics (PK) parameters between genotypes by the Kruskal–Wallis test. Although a monotone increasing pattern with a number of alleles is expected for PK-related genes, the Kruskal–Wallis test does not consider a monotonic response pattern. For detecting such patterns in clinical and toxicological trials, a maximum contrast method has been proposed. We show how that method can be used with pharmacogenomics data to a develop test of association. Further, using simulation studies, we compare the power of the modified maximum contrast method to those of the maximum contrast method and the Kruskal–Wallis test. On the basis of the results of those studies, we suggest rules of thumb for which statistics to use in a given situation. An application of all three methods to an actual genome-wide pharmacogenomics study illustrates the practical relevance of our discussion.
The Pharmacogenomics Journal (2009) **9**, 137–146; doi:10.1038/tpj.2008.17; published online 23 December 2008

Keywords: gemcitabine; genome-wide study; maximum contrast method; pharmacokinetics-related gene; statistical screening method

Introduction

Interindividual variation in drug response among patients is well known and poses a serious problem in medicine. The variation could be because of multiple factors such as disease phenotypes, genetic and environmental factors and the variability in drug target response (pharmacodynamic response) or allergic response, all factors that affect drug absorption, distribution, metabolism and excretion, side effects or efficacy.[1–3] However, at present, few biomarkers can predict, which group of patients will respond positively, which patients are nonresponders and who might experience adverse reactions for the same medication and dose. To realize personalized medicine, it is critically important to observe individual differences in drug response and the role of genetic polymorphisms that are relevant to the pathways of drug metabolism and the biology of drug responses in the pharmacogenomics of common diseases.[4]

With this background, the Food and Drug Administration (FDA) recognizes the importance of pharmacogenomics and has issued a guidance that encourages pharmacogenomics during drug development.[5] Many pharmacogenomics studies have been launched worldwide, such as a combination of a pharmaco-

kinetic (PK) study and analyses of single nucleotide polymorphisms (SNPs) in a candidate gene or in a genome-wide approach. Following the completion of the HapMap project,[6] the advent of the powerful array-based SNP typing platforms has heralded an era in which a genome-wide approach is a popular or standard strategy for identifying disease susceptibility or drug response genes for common diseases.[7–9]

To identify the SNPs, which relate to the pathways of drug metabolism, biomedical researchers usually test the null hypothesis (H_0) that there is no difference of the population mean of PK parameters (that is, area under the curve (AUC), maximum drug concentration (C_{max}), half-life period ($t_{1/2}$) and so on) between genotypes by using mainly the nonparametric analysis of variance, that is, the Kruskal–Wallis test.[10,11] On the basis of the statistical significance of the results from that test, researchers check the PK-genotype response patterns by sight, and then detect an additive, recessive or dominant model. The PK-related genes indicate a monotone increasing pattern in the number of alleles such as genetic models (additive, recessive and dominant pattern) as shown in Figure 1. Because a genome-wide association study is often designed as a multistage process, a relatively relaxed type I error rate is adopted in the first stage screening to assure the overall power of the study. If the Kruskal–Wallis test is applied to a significance level of $P=0.05$ in the first stage of a genome-wide association study, it is expected that as many as 5000–50 000 SNPs should be visually inspected for the current standard genome scan typing platform. Development of more objective and efficient screening method than the current subjective procedure is needed.

As a statistical method for detecting a monotonic dose–response relationship, a maximum contrast method has been proposed in clinical trials and toxicological trials.[12–17] This method, formed by taking the maximum over multiple contrast statistics for detecting a monotonic increase with the dose levels, is useful. The dose–response curves are modeled as the response patterns, and the set of contrast statistics is determined based on the set of contrast coefficients that correspond to these patterns. The contrast statistics should consist of contrast coefficients that are highly correlated with the population means for realistic dose–response relationships. The maximum contrast method is then applied to this set, and the pattern of the contrast coefficients for the contrast statistic that takes the maximum value is then selected as the true response pattern (see Materials and methods section).

In a typical pharmacogenomics study, the association of between PK parameter and genotype is modeled as the response patterns in Figure 1, and then the maximum contrast method is applied to this study on three contrast statistics with the following coefficients: $\boldsymbol{c}_1=(-1\ 0\ 1)^t$, $\boldsymbol{c}_2=(-2\ 1\ 1)^t$, $\boldsymbol{c}_3=(-1\ -1\ 2)^t$. The first contrast statistics corresponds to an additive model, the second to a recessive model and the third to a dominant model. As a result, the pattern of the coefficients for the contrast statistic that takes the maximum value is then selected as the true response pattern. However, the sample size of each genotype was enormously unbalanced, because the minor allele frequency (MAF) is less than 0.5, and the population is in Hardy–Weinberg equilibrium (HWE). Here we propose a modified maximum contrast method to detect an association between a PK parameter and genotype that accounts for the imbalance in genotype groups (see Materials and methods section).

In this paper, we proposed a modified maximum contrast method for detecting an association between PK parameter and genotype. Further, using simulation studies, we compare the Kruskal–Wallis test, the maximum contrast method and the modified maximum contrast method for pharmacogenomics data. We also suggest rules of thumb for

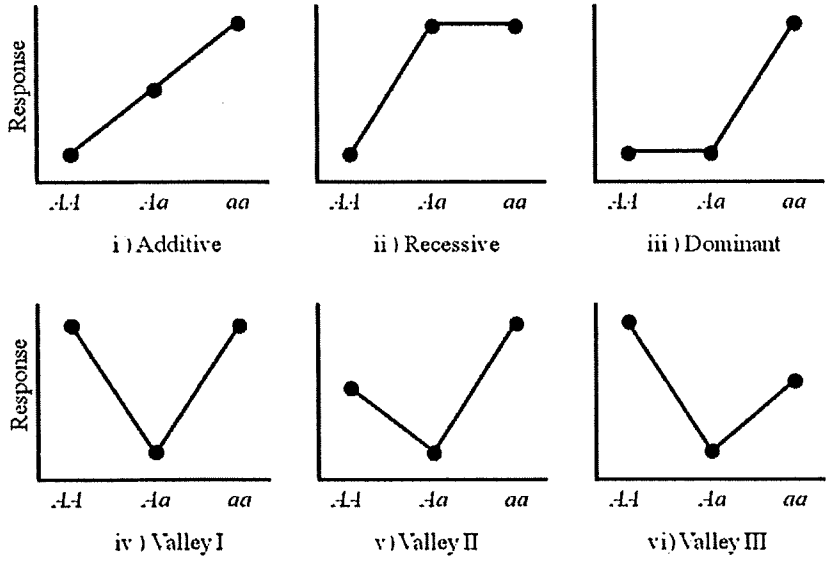

Figure 1 Pharmacokinetics parameter–genotype response patterns.

choosing a powerful maximum contrast statistic for such data. Finally, the discussed methodology is illustrated by its application to a pharmacogenomics study to antitumor drugs on Japanese cancer patients.

Results

Simulation study

To assess the power of the Kruskal–Wallis test, the maximum contrast method and the modified maximum contrast method, we first performed a Monte-Carlo simulation. Summary results of the simulation for each method are shown in Table 1 for various values of Δ and MAF when sample size (n) is set at 300. Note first that the diagonal box shows the positive predictive value (R_{TP}) for detection of true response patterns, whereas the row at the far right is the power (R_p) for detection of PK-related SNPs and includes the misidentification of true response patterns, where the result of R_{TP} by the Kruskal–Wallis test is blank because that test is an overall test and rejects the null hypothesis that there is no difference of the population mean of PK parameters. In a case where $\Delta = 0$, the R_p corresponds to a type I error rate of 5%, and is mostly controlled below 5%, but is inflated slightly for some models. The R_p and R_{TP} increase with increasing Δ; on the other hand, both R_p and R_{TP} decrease as the MAF decreases. We evaluated each method for detecting true response patterns. As a result, when the MAF is less than or equal to 0.25, in the additive and dominant pattern, the modified maximum contrast method is about 0.1–0.4 higher than the maximum contrast method in the R_{TP}. However, in the recessive model, the modified maximum contrast method is about 0.4 lower than the maximum contrast method in the R_{TP}. Therefore, under unbalanced sample size, the modified maximum contrast method is more powerful for detecting true response patterns than the maximum contrast method in the additive and dominant model, whereas the maximum contrast method is more powerful than the modified maximum contrast method in the recessive model.

For detecting PK-related genes, the Kruskal–Wallis test is lower in power than both maximum contrast methods in the R_p, under equivalent sample size (MAF = 0.5), whereas the Kruskal–Wallis test is about 0.05–0.10 higher in power than both maximum contrast methods under the unbalanced sample size (MAF $\leqslant$ 0.25). On the other hand, the R_p of the Kruskal–Wallis test is about 0.10–0.50 higher than both maximum contrast methods under the simulation condition without the PK-related SNPs in Table 2. Therefore the simulation studies suggest that the Kruskal–Wallis test detects many PK-nonrelated SNPs because of not considering the response patterns.

Questionnaire survey on judgment

We next conducted a questionnaire survey to compare the judgment by each statistical method (modified maximum contrast method and maximum contrast method) with the judgment by experts. The results are shown in Table 3. For the recessive and no-response pattern, the judgment of both statistical methods well accords with the judgment by expert. For the additive and dominant pattern, the maximum contrast method detects as a recessive pattern by mistake, and the modified maximum contrast method well accords with the judgment by expert. The Kendall's rank correlation coefficient between modified maximum contrast method and expert's judgment is 0.731; on the other hand, the correlation coefficient between the maximum contrast method and expert's judgment is 0.423. The conclusion is that the judgment of modified maximum contrast method is closer to the judgment by expert than is the maximum contrast method.

Application to actual genome-wide pharmacogenomics study

In this paper, we focus on the elimination rate constant (K_{el}), which is the first order rate constant describing drug elimination from the body, and report the results of PK-related SNPs associated with K_{el}. The histogram for the K_{el} is shown in Figure 2. The PK data seem to be skewed to the left tail of the distribution; therefore we transformed data before applying both maximum contrast methods by taking the natural logarithm of the observed values.

Table 4 summarizes the number of significant SNPs for various P-value cutoffs by each method. For the P-value cutoff of 0.001, 84 SNPs are significant by the Kruskal–Wallis test, 77 SNPs by the maximum contrast method and 84 SNPs by the modified maximum contrast method. Two SNPs (GLT25D1: rs3848643 and BCNP1: rs6512201) are detected as additive model by all three methods in Table 5. In considering a multiple testing problem, we assume the existence of about 10 000 linkage disequilibrium blocks within 100 000 gene-centric SNPs, which are concentrated in about 2% of the human genome (that is, average interval of two SNPs is 600 bp). It follows that the P-value cutoff is set at 5.0×10^{-6} as Bonferroni correlation. As a result, two SNPs (rs2148582, rs699) in angiotensinogen (*AGT*) gene are detected as a dominant model by both the maximum contrast method and modified maximum contrast method, but no SNPs are detected by the Kruskal–Wallis test. We show all of the results for association between PK parameters and SNPs at Genome Medicine Database of Japan (http://gemdbj.nibio.go.jp).

Discussion

We reviewed the current methodology for analyzing PK-SNP data in pharmacogenomics studies. We proposed a modified maximum contrast method for detecting a PK-genotype response pattern under unbalanced sample size. The simulation study suggested that both the maximum contrast method and the modified maximum contrast method were more useful for screening PK-related SNPs in consideration of genetic models than is the Kruskal–Wallis test, and that under unbalanced sample size, the modified maximum contrast method was more powerful for detecting true response patterns than the maximum contrast method in the additive and dominant pattern, whereas the maximum contrast method is more powerful than the modified maximum contrast method in the recessive model.

Table 1 The R_p and R_{TP} for various response patterns

Δ	MAF	True situation		Judgment			
				Additive	Recessive	Dominant	R_P
0			MMCM	0.007	0.017	0.023	0.047
		Additive	MCM	0.007	0.017	0.023	0.047
			K–W	—	—	—	0.049
			MMCM	0.008	0.017	0.017	0.042
	0.50	Recessive	MCM	0.008	0.017	0.017	0.042
			K–W	—	—	—	0.045
			MMCM	0.015	0.024	0.022	0.061
		Dominant	MCM	0.015	0.024	0.023	0.062
			K–W	—	—	—	0.052
			MMCM	0.008	0.002	0.043	0.053
		Additive	MCM	0.009	0.024	0.021	0.054
			K–W	—	—	—	0.051
			MMCM	0.008	0.002	0.043	0.053
	0.25	Recessive	MCM	0.011	0.031	0.019	0.061
			K–W	—	—	—	0.048
			MMCM	0.006	0.000	0.051	0.057
		Dominant	MCM	0.014	0.014	0.023	0.051
			K–W	—	—	—	0.039
			MMCM	0.001	0.000	0.035	0.036
		Additive	MCM	0.004	0.026	0.018	0.048
			K–W	—	—	—	0.050
			MMCM	0.002	0.000	0.042	0.044
	0.12	Recessive	MCM	0.009	0.018	0.017	0.044
			K–W	—	—	—	0.055
			MMCM	0.000	0.000	0.048	0.048
		Dominant	MCM	0.008	0.018	0.025	0.051
			K–W	—	—	—	0.043
0.5			MMCM	0.405	0.140	0.144	0.689
		Additive	MCM	0.408	0.138	0.144	0.690
			K–W	—	—	—	0.628
			MMCM	0.130	0.672	0.005	0.807
	0.50	Recessive	MCM	0.128	0.674	0.005	0.807
			K–W	—	—	—	0.772
			MMCM	0.134	0.012	0.679	0.825
		Dominant	MCM	0.133	0.011	0.682	0.826
			K–W	—	—	—	0.769
			MMCM	0.211	0.041	0.139	0.391
		Additive	MCM	0.135	0.373	0.030	0.538
			K–W	—	—	—	0.452
			MMCM	0.173	0.308	0.009	0.490
	0.25	Recessive	MCM	0.009	0.747	0.001	0.757
			K–W	—	—	—	0.789
			MMCM	0.063	0.000	0.413	0.476
		Dominant	MCM	0.134	0.066	0.238	0.438
			K–W	—	—	—	0.381
			MMCM	0.036	0.002	0.106	0.144
		Additive	MCM	0.043	0.192	0.010	0.245
			K–W	—	—	—	0.267
			MMCM	0.089	0.017	0.027	0.133
	0.12	Recessive	MCM	0.004	0.443	0.001	0.448
			K–W	—	—	—	0.593
			MMCM	0.010	0.000	0.192	0.202
		Dominant	MCM	0.058	0.058	0.072	0.188
			K–W	—	—	—	0.165
1.0			MMCM	0.966	0.019	0.012	0.997
		Additive	MCM	0.968	0.018	0.011	0.997
			K–W	—	—	—	0.998

Table 1 *Continued*

Δ	MAF	True situation		Judgment			
				Additive	*Recessive*	*Dominant*	R_P
			MMCM	0.004	0.996	0.000	1.000
	0.5	Recessive	MCM	0.004	0.996	0.000	1.000
			K–W	—	—	—	1.000
			MMCM	0.002	0.000	0.998	1.000
		Dominant	MCM	0.002	0.000	0.998	1.000
			K–W	—	—	—	1.000
			MMCM	0.764	0.133	0.053	0.950
		Additive	MCM	0.395	0.592	0.001	0.988
			K–W	—	—	—	0.980
			MMCM	0.052	0.944	0.000	0.996
	0.25	Recessive	MCM	0.000	1.000	0.000	1.000
			K–W	—	—	—	1.000
			MMCM	0.042	0.000	0.934	0.976
		Dominant	MCM	0.195	0.041	0.724	0.960
			K–W	—	—	—	0.920
			MMCM	0.390	0.014	0.121	0.525
		Additive	MCM	0.071	0.708	0.003	0.782
			K–W	—	—	—	0.818
			MMCM	0.185	0.485	0.001	0.671
	0.12	Recessive	MCM	0.000	0.964	0.000	0.964
			K–W	—	—	—	0.994
			MMCM	0.033	0.000	0.624	0.657
		Dominant	MCM	0.175	0.151	0.319	0.645
			K–W	—	—	—	0.483

Abbreviations: Δ, given coefficient of response mean value; K–W, Kruskal–Wallis test; MAF, minor allele frequency; MCM, maximum contrast method; MMCM, modified maximum contrast method.
Notation for defining R_P and R_{TP}.
Positive predictive value: $R_{TP} = N_{TP}/N$, power: $R_P = N_R/N$.
Shaded region shows the positive predictive value (R_{TP}) for detection of true response patterns.

In addition, the survey on judgment for PK-related SNPs makes evident that the modified maximum contrast method gave a judgment closer to the judgment of experts than did the maximum contrast method. The expert's judgment was subjective, and also different by each expert. The modified maximum contrast method and the maximum contrast method were able to objectively detect the response pattern and the PK-related SNPs under unbalanced sample size.

The application of the maximum contrast method, modified maximum contrast method and Kruskal–Wallis test to a pharmacogenomics study supported these considerations. When the *P*-value cutoff was set at 0.05 in this application, about 5000 SNPs were detected as statistical significance, and both maximum contrast methods were able to show each genetic model to the biomedical researcher. We showed the list of identified SNPs by each method. The two SNPs in the *AGT* gene showed a statistical significant difference in K_{el} by both the maximum contrast method and modified maximum contrast method, but the Kruskal–Wallis test was not able to detect the gene after multiple testing adjustment. Polymorphic variations in the human *AGT* gene have been shown to be associated with

Table 2 False positive for response patterns

Δ	MAF	Response pattern	K–W	MCM	MMCM
0.5	0.5	Valley I	0.780	0.467	0.455
		Valley II	0.617	0.519	0.513
		Valley III	0.623	0.543	0.540
	0.25	Valley I	0.765	0.304	0.177
		Valley II	0.355	0.259	0.311
		Valley III	0.713	0.493	0.227
	0.12	Valley I	0.515	0.184	0.087
		Valley II	0.213	0.124	0.149
		Valley III	0.546	0.272	0.071
1.0	0.5	Valley I	1.000	0.989	0.987
		Valley II	0.999	0.995	0.995
		Valley III	0.998	0.992	0.991
	0.25	Valley I	1.000	0.937	0.774
		Valley II	0.924	0.746	0.797
		Valley III	1.000	0.988	0.890
	0.12	Valley I	0.991	0.579	0.243
		Valley II	0.687	0.346	0.404
		Valley III	0.996	0.800	0.298

Abbreviations: Δ, given coefficient of response mean value; K–W, Kruskal–Wallis test; MAF, minor allele frequency; MCM, maximum contrast method; MMCM, modified maximum contrast method.

Table 3 Difference in judgment between statistical methods and experts

Modified maximum contrast method		*Maximum contrast method*		*Expert*
P-value	*Judgment*	*P-value*	*Judgment*	*Judgment*
0.007	Additive	<0.00001	Recessive	Additive (5), dominant (1)
0.009	Additive	0.014	Additive	Additive (4), dominant (1), recessive (1)
0.003	Recessive	0.004	Recessive	Recessive (4), additive (1), dominant (1)
0.011	Dominant	0.008	Dominant	Dominant (4), none (2)
<0.00001	Dominant	0.001	Recessive	Dominant (6)
0.998	None	0.999	None	None (6)

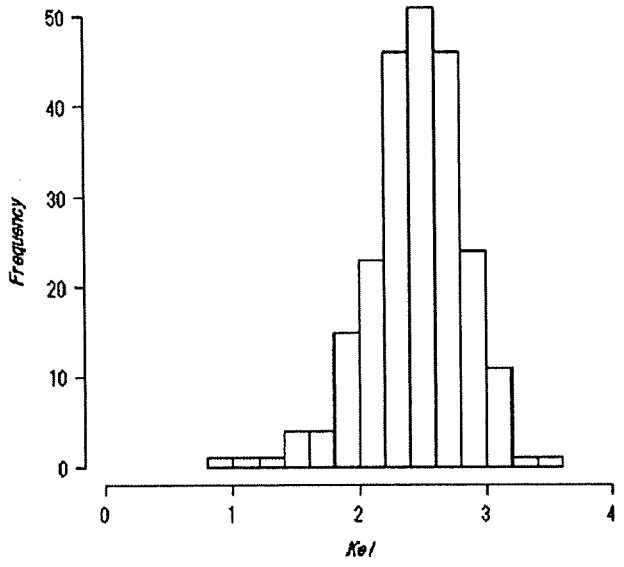

Figure 2 Histogram of elimination rate constant (K_{el}) for the gemcitabine pharmacogenomic (PGx) study.

Table 4 Number of significant SNPs for various *P*-value cutoffs by each method

P-value cutoff	*Method*	*Additive*	*Recessive*	*Dominant*	*Total*
$P \leqslant 0.05$	K–W	—	—	—	4295 SNPs
	MCM	829 SNPs	1768 SNPs	1777 SNPs	4374 SNPs
	MMCM	705 SNPs	239 SNPs	3471 SNPs	4415 SNPs
$P \leqslant 0.01$	K–W	—	—	—	774 SNPs
	MCM	175 SNPs	304 SNPs	385 SNPs	864 SNPs
	MMCM	117 SNPs	51 SNPs	716 SNPs	884 SNPs
$P \leqslant 0.005$	K–W	—	—	—	369 SNPs
	MCM	105 SNPs	146 SNPs	182 SNPs	433 SNPs
	MMCM	59 SNPs	17 SNPs	377 SNPs	453 SNPs
$P \leqslant 0.001$	K–W	—	—	—	84 SNPs
	MCM	16 SNPs	27 SNPs	34 SNPs	77 SNPs
	MMCM	11 SNPs	0 SNPs	73 SNPs	84 SNPs
$P \leqslant 0.0005$	K–W	—	—	—	47 SNPs
	MCM	8 SNPs	15 SNPs	27 SNPs	50 SNPs
	MMCM	6 SNPs	0 SNPs	45 SNPs	51 SNPs
$P \leqslant 0.0001$	K–W	—	—	—	6 SNPs
	MCM	3 SNPs	5 SNPs	9 SNPs	17 SNPs
	MMCM	3 SNPs	0 SNPs	17 SNPs	20 SNPs

Abbreviations: K–W, Kruskal–Wallis test; MCM, maximum contrast method; MMCM, modified maximum contrast method; SNPs, single nucleotide polymorphisms.

increased circulating AGT concentrations,[18] an increased risk of essential hypertension,[18–22] and a decline in renal function.[23] Although it is possible that the *AGT* gene polymorphisms influence gemcitabine PK through yet unknown mechanisms, the result and the suggested hypothesis in our study should be evaluated both in replication study using another sample set and also in biological functional analyses.

Many biomedical researchers have used the Kruskal–Wallis test for finding significant SNPs, and visually checked PK-genotype response patterns. Recently, powerful array-based SNP typing platforms have heralded an era in which a genome-wide association study is a popular or standard strategy for identifying disease associated genes or drug response genes for common diseases, and genotype data on 100 000–1 000 000 SNPs are increasingly available to researchers. It is virtually impossible for biomedical researchers to visually check the response patterns on such a genome scan data. Our study has proposed an alternative by showing that either a modified maximum contrast method or a maximum contrast method can readily be applied to genome scans as a statistical screening method.

Materials and methods

Maximum contrast method and modified maximum contrast method

We first describe a general form for a maximum contrast method as discussed in Yoshimura *et al.*,[14] and Wakana *et al.*,[17] in a pharmacogenomics study. We assume Y_{ij} ($i = 1, 2, 3$; $j = 1, 2, \ldots, n_i$) as an observed response for jth individual in ith genotype group (*AA*, *Aa* and *aa*, where '*A*' is major

Table 5 List of identified SNPs by each method

Gene information				*K–W*	*MCM*		*MMCM*	
Chr	*RS #*	*Allele*	*Gene*	*P-value*	*P-value*	*Pattern*	*P-value*	*Pattern*
1	rs2148582	A/G	*AGT*	0.011	1.5×10^{-9}	Dominant	8.6×10^{-7}	Dominant
1	rs699	C/T	*AGT*	0.012	1.5×10^{-9}	Dominant	1.4×10^{-6}	Dominant
3	rs1132979	C/G	*eIF2A*	4.1×10^{-4}	2.7×10^{-4}	Additive	1.0×10^{-4}	Dominant
4	rs11736926	C/G	*NDST4*	0.0046	3.4×10^{-4}	Dominant	1.0×10^{-4}	Dominant
6	rs1932523	A/G	*FILIP1*	0.0073	2.7×10^{-4}	Dominant	1.0×10^{-4}	Dominant
6	rs2223869	C/T	*TFAP2B*	8.8×10^{-5}	0.25	Recessive	0.48	Recessive
6	rs2703702	A/G	*FILIP1*	0.0027	1.0×10^{-4}	Dominant	1.0×10^{-4}	Dominant
7	rs12667496	C/T	*HIC*	0.0070	8.9×10^{-6}	Recessive	0.0015	Dominant
8	rs2938303	A/G	*OXR1*	4.2×10^{-4}	1.0×10^{-4}	Additive	1.0×10^{-4}	Additive
9	rs4149336	C/T	*ABCA1*	0.0049	3.3×10^{-4}	Dominant	2.8×10^{-4}	Dominant
9	rs4842151	C/T	*COL5A1*	2.7×10^{-5}	5.2×10^{-5}	Recessive	0.0032	Additive
9	rs4842152	C/T	*COL5A1*	8.4×10^{-5}	7.6×10^{-5}	Recessive	0.0023	Additive
12	rs4763797	A/G	*LRP6*	0.033	2.4×10^{-5}	Dominant	1.0×10^{-4}	Dominant
14	rs1243459	C/T	*C14orf8*	0.003	1.7×10^{-4}	Dominant	1.0×10^{-4}	Dominant
15	rs2271714	A/G	*MFGE8*	0.002	1.0×10^{-4}	Dominant	1.0×10^{-4}	Dominant
17	rs2233362	A/G	*GNGT2*	3.5×10^{-4}	2.0×10^{-4}	Dominant	1.0×10^{-4}	Dominant
18	rs12607882	C/T	*METTL4*	5.0×10^{-5}	0.057	Recessive	0.28	Recessive
19	rs3848643	C/T	*GLT25D1*	6.8×10^{-5}	8.1×10^{-5}	Additive	6.2×10^{-5}	Additive
19	rs6512201	C/G	*BCNP1*	5.2×10^{-5}	5.3×10^{-5}	Additive	4.3×10^{-5}	Additive
21	rs9647237	C/T	*C21orf12*	0.042	2.0×10^{-8}	Dominant	4.4×10^{-5}	Dominant
22	rs1008530	C/T	*TFIP11*	0.0018	2.0×10^{-4}	Dominant	1.0×10^{-4}	Dominant
22	rs1894704	A/C	*HPS4*	4.9×10^{-4}	1.8×10^{-5}	Dominant	1.0×10^{-4}	Dominant
22	rs1894705	C/T	*HPS4*	5.7×10^{-4}	1.3×10^{-5}	Recessive	3.1×10^{-4}	Dominant
22	rs3752589	G/T	*HPS4*	5.7×10^{-4}	1.4×10^{-5}	Recessive	3.1×10^{-4}	Dominant
22	rs5761557	A/G	*HPS4*	5.7×10^{-4}	1.1×10^{-5}	Recessive	1.0×10^{-4}	Dominant
22	rs713998	A/G	*HPS4*	4.9×10^{-4}	2.2×10^{-5}	Dominant	1.1×10^{-5}	Dominant
22	rs737800	C/T	*HPS4*	3.9×10^{-4}	3.4×10^{-5}	Dominant	1.0×10^{-4}	Dominant

Abbreviations: Chr, chromosome number; K–W, Kruskal–Wallis test; MCM, maximum contrast method; MMCM, modified maximum contrast method; RS#, dbSNP reference SNP identification number.
Shaded region is the identified SNPs by each method (*P*-value$\leqslant$0.0001).

allele, and '*a*' is minor allele), and Y_{ij}s are independently and normally distributed with $E(Y_{ij}) = \mu_i$ and $\mathrm{Var}(Y_{ij}) = \sigma^2$. Under these conditions, $\bar{\boldsymbol{Y}} = (\bar{Y}_1, \bar{Y}_2, \bar{Y}_3)^t$ follows the trivariate normal distribution $N(\mu, \sigma^2 D)$ where

$$\bar{Y}_i = \frac{1}{n_i}\sum_{j=1}^{n_i} Y_{ij},\ \boldsymbol{\mu} = (\mu_1, \mu_2, \mu_3)^t \quad \text{and}$$

$$\boldsymbol{D} = \mathrm{diag}\left(\frac{1}{n_1}, \frac{1}{n_2}, \frac{1}{n_3}\right),$$

diag(●) being a diagonal matrix, and the superscript t indicates the transpose of a matrix or vector. In the maximum contrast method, some contrast statistics are set according to the approach. Let contrast statistic T_k with a coefficient $\boldsymbol{c_k} = (c_{k1}, c_{k2}, c_{k3})^t$ where $c_{k1} + c_{k2} + c_{k3} = 0$, and $k = 1$, 2 and 3 correspond to an additive, recessive and dominant response pattern, respectively, as shown in Figure 1. The following coefficients were used for each genetic model:

$$c_1 = (-1 \quad 0 \quad 1)^t,$$
$$c_2 = (-2 \quad 1 \quad 1)^t,$$
$$c_3 = (-1 \quad -1 \quad 2)^t.$$

The contrast statistics is defined in terms of the contrast vector c_k,

$$T_k = \frac{c_k^t \bar{Y}}{\sqrt{\hat{\sigma}^2 c_k^t D c_k}}, \tag{1}$$

where $\hat{\sigma}^2$ is $\frac{1}{\gamma}\sum_{i=1}^{3}\sum_{j=1}^{n_i}(y_{ij} - \bar{y}_i)^2$, and $\gamma = \sum_{i=1}^{3} n_i - 3$ is degree of freedom of $\hat{\sigma}^2$. Then the statistic is defined as:

$$T_{\max} = \max(T_1, T_2, T_3). \tag{2}$$

The statistics can be used to test over null hypotheses, H_0: $\mu_1 = \mu_2 = \mu_3$, on the other hand, in pharmacogenomics studies, alternative hypotheses such as H_1: $\mu_1 < \mu_2 < \mu_3$, $\mu_1 = \mu_2 < \mu_3$, $\mu_1 < \mu_2 = \mu_3$. The *P*-value for the probability distribution of $T_{\max}$ under the over null hypotheses is calculated by using the complex property of integration in the multivariate *t*-distribution with singular correlation matrix,[24] and the *P*-value is defined as in the following formula:

$$\begin{aligned} P\text{-value} &= \Pr(t_{\max} > t^*_{\max} | H_0) = 1 - \Pr(t_{\max} \geqslant t^*_{\max}) \\ &= 1 - \Pr(t_1 < t^*_{\max},\ t_2 < t^*_{\max},\ t_3 < t^*_{\max}) \end{aligned}, \tag{3}$$

where $t^*_{\max}$ is the observed value of the test statistics.

This method can select the response pattern, which best fits the observed data among a set of patterns. In clinical and

toxicological trials, the sample size of each group is almost equivalent; therefore the maximum contrast method assumes an equivalent sample size of each group. However, the sample size of each group is not equivalent in pharmacogenomics studies, because the MAF is less than 0.5 and is generally around 0.2. For this reason, under the unbalanced sample size, the adjoining denominator of contrast statistic $\sqrt{\left(\frac{c_{k1}^2}{n_1}+\frac{c_{k2}^2}{n_2}+\frac{c_{k3}^2}{n_3}\right)\hat{\sigma}^2}$ is overestimated although the studentized statistics by this variance estimate is robust. Therefore, the maximum contrast method cannot be applied for detecting a true response pattern in pharmacogenomics studies.

Here we propose a modified maximum contrast method for unbalanced sample size. First, the modified contrast statistic is given by

$$T'_k = \frac{c_k^t \bar{Y}}{\sqrt{c_k^t c_k}}, \tag{4}$$

thus the adjoining denominator of the modified contrast statistic is $\sqrt{c_{k1}^2 + c_{k2}^2 + c_{k3}^2}$, and it is not influenced by unbalanced sample size. The modified maximum contrast statistic is given by

$$T'_{\max} = \max(T'_1, T'_2, T'_3). \tag{5}$$

In addition, the multiplicity adjusted *P*-value for the probability distribution of $T'_{\max}$ under H_0 was calculated by the permutation procedure.[25] Simple random sampling without replacement method generates the sampling distribution of the statistic by drawing repeated samples from the observed sample itself. Consequently, the permutation procedure is used to simulate *P*-values; the lowest *P*-value is calculated for each of 100 000 permutations for the entire dataset, and from this distribution.

Simulation study

We assess the power of the Kruskal–Wallis test, the maximum contrast method (Equations (1) and (2)) and the modified maximum contrast method (Equations (4) and (5)) by simulation studies. The scenarios discussed here are motivated by the anticancer drug's pharmacogenomics data that will be introduced below. In particular, we are interested in the performance of all three tests when the MAF decreases. To examine these effects, we simulate PK parameter data from transformed log-normal distribution by each genotype. The distributions of PK parameters are often unknown, but empirically are modeled under the assumption of a log-normal distribution because (1) PK parameter values must be nonnegative and the normal assumption does not enforce this assumption; (2) distribution of estimated PK parameters is often left skewed, which is compatible with a log-normal distribution.[26] Here, for applying an intravenous anticancer drug in actual data, we focus on the elimination rate constant (K_{el}), which is the first order rate constant describing drug elimination from the body. We assume that a sample of patients with any genotype (*AA*, *Aa* or *aa*) and the proportion of MAF is given, and that this population is in HWE. For each patient, the PK parameter, K_{el} is given. Under these assumptions, we generated K_{el} by each genotype from the log-normal distribution with mean μ_i, that is, $\bar{Y}_i \sim \mathrm{LN}(\mu_i, 1)$, $i=1, 2, 3$ in *i*th genotype group (*AA*, *Aa* and *aa*), where $\mu_i = \Delta \cdot c_{ki}$ and Δ is given coefficient and c_{ki} corresponded to element of contrast statistics vector $\boldsymbol{c_k} = (c_{k1}\ c_{k2}\ c_{k3})^t$. Here, Δ is set at 0.0, 0.5 and 1.0, respectively, and the contrast statistics vectors are set as the following coefficients corresponding to the genetic models ($k=1$, 2 and 3) in Figure 1 (i)–(iii):

$$\boldsymbol{c}_1 = (-1\ \ 0\ \ 1)^t,$$
$$\boldsymbol{c}_2 = (-2\ \ 1\ \ 1)^t,$$
$$\boldsymbol{c}_3 = (-1\ \ -1\ \ 2)^t.$$

In addition, the MAF was set at 0.12, 0.25 or 0.50, respectively, where total sample size (n) was 300 or 600 subjects. The criteria to evaluate the performance of each method were two indicators, R_P and R_{TP}, defined by Equations (6) and (7).

$$R_P = \frac{N_R}{N}, \tag{6}$$

$$R_{TP} = \frac{N_{TP}}{N}. \tag{7}$$

R_P is a proportion of detected PK-related SNPs (power), whereas R_{TP} is the proportion of detected true response patterns among PK-related SNPs (positive predictive value). The Monte-Carlo simulation to calculate R_P and R_{TP} was repeated 10 000 times and the mean values of indicators were calculated. Note that N was a constant fixed as the repetition number of the simulation, whereas N_R was a random variable realized as the number of rejections by the hypothesis test, and N_{TP} was the number of detected true response patterns.

Questionnaire survey on judgment

To identify PK-related genes, biological experts who are pharmacokinetists, molecular biologists and geneticists used to draw box-and-whisker plots on PK parameters by each genotype, and check these response patterns by sight. This judgment involves much experience, but it is subjective and may differ by expert. We conducted a questionnaire survey to compare statistical judgment with judgment by experts. First, we showed summary statistics and box–whisker plot (Figure 3) to the expert group that consisted of two pharmacokinetists, two molecular biologists and two geneticists. Second, these experts independently gave a decision from six response patterns (Figure 1). Finally, we applied the modified maximum contrast method and the maximum contrast method to this survey dataset, and, by using Kendall's rank correlation coefficient, evaluated, which method is closer to expert judgment.

Application to actual gemcitabine pharmacogenomics study

We applied the Kruskal–Wallis test, the maximum contrast method and the modified maximum contrast method to an actual genome-wide pharmacogenomics study on antitumor drugs. The study was performed within the Millennium Genome Project in Japan, and four antitumor drugs were